

Biocompatible Graphene Oxide-Based Glucose Biosensors

Yong Liu,^{*,†} Dingshan Yu,[‡] Chao Zeng,[†] Zongcheng Miao,[§] and Liming Dai^{*,†,‡}

[†]Biomedical Engineering Academy, School of Ophthalmology & Optometry, Wenzhou Medical College, 270 Xueyuan Road, Wenzhou 325027, China, [‡]Department of Chemical Engineering, Case Western Reserve University, 10900 Euclid Avenue, Cleveland, Ohio 44106, and [§]College of Chemistry and Chemical Engineering, Shaan-xi University of Science and Technology, Xi-an 710021, China

Received March 3, 2010. Revised Manuscript Received March 21, 2010

This letter demonstrates that a novel, highly efficient enzyme electrode can be directly obtained using covalent attachment between carboxyl acid groups of graphene oxide sheets and amines of glucose oxidase. The resulting biosensor exhibits a broad linear range up to $28 \text{ mM} \cdot \text{mm}^{-2}$ glucose with a sensitivity of $8.045 \text{ mA} \cdot \text{cm}^{-2} \cdot \text{M}^{-1}$. The glucose oxidase-immobilized graphene oxide electrode also shows a reproducibility and a good storage stability, suggesting potentials for a wide range of practical applications. The biocompatibility of as-synthesized graphene oxide nanosheets with human cells, especially retinal pigment epithelium (RPE) cells, was investigated for the first time in the present work. Microporous graphene oxide exhibits good biocompatibility and has potential advantages with respect to cell attachment and proliferation, leading to opportunities for using graphene-based biosensors for the clinical diagnosis.

Owing to their unique electrical, thermal, and mechanical properties, graphene and its derivatives, including graphene oxide (GO), have attracted ever increasing attention in recent years as a novel class of 2D carbon-based nanomaterials.¹ Of particular interest is that GO nanosheets are soluble in water and many other common polar solvents with respect to the formation of large-scale uniform films on various substrates. Subsequent thermal annealing of the GO films under a hydrogen atmosphere has been demonstrated to produce graphene sheets, which otherwise are difficult to produce because of their poor processability.^{2–6} The direct application of GO in electrically active materials and devices, however, is still limited by the high electrical resistance associated with the presence of carboxyl, hydroxyl, or epoxy groups in GO sheets, as schematically shown in Figure 1a.⁷

On the other hand, the presence of oxygen-containing functional groups provides potential advantages to GO for numerous applications because they can be used to introduce multifunctionalities. For example, Li et al. demonstrated the electrostatic stabilization of GO colloids via carboxylic acid groups in the GO sheet.⁸ Because of their interesting electrochemical behavior, carbon materials including glassy carbon,⁹ carbon paste,¹⁰ gra-

phite,¹¹ carbon fibers,¹² fullerenes,¹³ carbon nanotubes,^{14,15} nanodiamonds,¹⁶ and even functionalized graphene nanomaterials^{17–19} have been well studied for enzyme immobilization and biosensor applications. Here, we present a direct, simple way to utilize the carboxyl groups of GO as a target for the immobilization of enzyme. The resulting biosensors have been demonstrated to exhibit a linear response over a broad concentration range up to $28 \text{ mM} \cdot \text{mm}^{-2}$ glucose with a sensitivity of about $8 \text{ mA} \cdot \text{cm}^{-2} \cdot \text{M}^{-1}$. These GO-based glucose sensors also showed excellent reproducibility and good operation/storage stability, suggesting great potential for a wide range of practical applications. The as-synthesized GO nanosheets further exhibited good biocompatibility to human RPE cells, indicating potential applications for in-vivo clinical diagnosis of diseases such as diabetic retinopathy.

In a typical experiment, GO is prepared on a Pt disk electrode (i.d. 1 mm) as described in the Supporting Information. As schematically shown in Figure 1c, the amine groups of glucose oxidase (GOx) were covalently attached to the carboxyl acid groups of GO in the presence of 1-ethyl-3-(3-dimethylaminopropyl) carbodiimide hydrochloride (EDC) and *N*-hydroxyl succinimide (NHS).²⁰

The morphology of the as-prepared GO sheet is determined using an atomic force microscope (AFM) in a tipping mode. The AFM micrograph of GO shows that the thickness of the resulting GO sheets is approximately 1.2 nm, suggesting that the GO film

*Corresponding authors. E-mail: yongliu1980@hotmail.com, liming.dai@case.edu.

- (1) Geim, A. K.; Novoselov, K. S. *Nat. Mater.* **2007**, *6*, 183.
- (2) Stankovich, S.; Dikin, D. A.; Dommett, G. H. B.; Kohlhaas, K. M.; Zimney, E. J.; Stach, E. A.; Piner, R. D.; Nguyen, S. T.; Ruoff, R. S. *Nature* **2006**, *442*, 282.
- (3) Dikin, D. A.; Stankovich, S.; Zimney, E. J.; Piner, R. D.; Dommett, G. H. B.; Evmenenko, G.; Nguyen, S. T.; Ruoff, R. S. *Nature* **2007**, *448*, 457.
- (4) Eda, G.; Fanchini, G.; Chhowalla, M. *Nat. Nanotechnol.* **2008**, *3*, 270.
- (5) Gomez-Navarro, C.; Weitz, R. T.; Bittner, A. M.; Scolari, M.; News, A.; Burghard, M.; Kern, K. *Nano Lett.* **2007**, *7*, 3499.
- (6) Ramanathan, T.; Abdala, A. A.; Stankovich, S.; Dikin, D. A.; Herrera-Alonso, M.; Piner, R. D.; Adamson, D. H.; Schniepp, H. C.; Chen, X.; Ruoff, R. S.; Nguyen, S. T.; Aksay, I. A.; Prud'Homme, R. K.; Brinson, L. C. *Nat. Nanotechnol.* **2008**, *3*, 327.
- (7) Mkhoyan, K. A.; Contryman, A. W.; Silcox, J.; Stewart, D. A.; Eda, G.; Mattevi, C.; Miller, S.; Chhowalla, M. *Nano Lett.* **2009**, *9*, 1058.
- (8) Li, D.; Müller, M. B.; Gilje, S.; Kaner, R. B.; Wallace, G. G. *Nat. Nanotechnol.* **2008**, *3*, 101.
- (9) Cosnier, S.; Fombon, J. J.; Labbé, P.; Limosin, D. *Sens. Actuators, B* **1999**, *59*, 134.
- (10) Kulys, J. *Biosens. Bioelectron.* **1999**, *14*, 473.
- (11) Horozova, E.; Dimcheva, N.; Jordanova, Z. *Bioelectrochemistry* **2000**, *53*, 11.

- (12) Netchiporouk, L. I.; Shul'ga, A. A.; Jaffrezic-renault, N.; Martelet, C.; Olier, R.; Cespuccio, R. *Anal. Chim. Acta* **1995**, *303*, 275.
- (13) Nednoor, P.; Capaccio, M.; Gavalas, V. G.; Meier, M. S.; Anthony, J. E.; Bachas, L. G. *Bioconjugate Chem.* **2004**, *15*, 12.
- (14) Poh, W. C.; Loh, K. P.; Zhang, W. D.; Sudhiranjan, T.; Ye, J. S.; Sheu, F. S. *Langmuir* **2004**, *20*, 5484.
- (15) Liu, Y.; Chen, J.; Anh, N. T.; Too, C. O.; Misoska, V.; Wallace, G. G. *J. Electrochem. Soc.* **2008**, *155*, K100.
- (16) Zhao, W.; Xu, J. J.; Liu, Q. Q.; Chen, H. Y. *Biosens. Bioelectron.* **2006**, *22*, 649.
- (17) Yang, S.; Guo, D.; Su, L.; Yu, P.; Li, D.; Ye, J.; Mao, L. *Anal. Chem.* **2009**, *81*, 5603.
- (18) Shan, C.; Yang, H.; Song, J.; Han, D.; Ivaska, A.; Niu, L. *Anal. Chem.* **2009**, *81*, 2378.
- (19) Lu, C.; Yang, H.; Zhu, C.; Chen, X.; Chen, G. *Angew. Chem., Int. Ed.* **2009**, *48*, 4785.
- (20) Lin, Y. H.; Lu, F.; Tu, Y.; Ren, Z. F. *Nano Lett.* **2004**, *4*, 191.

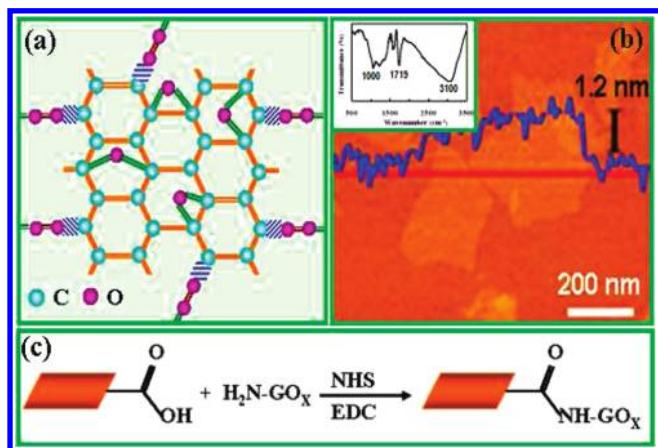


Figure 1. (a) Schematic representation of the molecular structure of a GO sheet, (b) AFM micrograph of the GO sheets, and (c) schematic immobilization of GOx into GO sheets via peptide bonds between the amine groups of GOx and the carboxylic acid of GO. (b, Inset) FTIR spectrum of GO.

consists of a single layer (Figure 1b). The corresponding infrared (IR) spectrum given in the inset of Figure 1b shows a broad band at 3100 cm^{-1} associated with the absorption of hydroxyl group. A strong band at 1719 cm^{-1} can be attributed to the presence of carboxyl groups. The band obtained at 1000 cm^{-1} arises from the stretching vibration of C–O.

Figure S1 shows cyclic voltammograms (CVs) of the GOx–GO electrode in $10\text{ mM K}_4\text{Fe(CN)}_6/0.4\text{ M}$ phosphate buffer solution (PBS, pH 7.4) at a scan rate of 50 mV s^{-1} compared with the pristine GO electrode. A couple of well-defined redox peaks were both found at the GO electrode (pink line) and the GO electrode after the immobilization of GOx (blue line). During cyclic voltammetry, GO was electroreduced, giving rise to the electroactive performance of the electrode in $\text{K}_4\text{Fe(CN)}_6$ whereas the reduction process is electrochemically irreversible as reported elsewhere.²¹ Smaller peak currents and a wider peak potential separation (ΔE_p) are observed at the GOx–GO electrode, suggesting the lower electron transfer of the electrode after the incorporation of GOx. This can be attributed to the native low electron-transfer rates of GOx.¹⁶

Amperometry has been considered to be an efficient method of determining the performance of a glucose biosensor.²² A constant potential ($+0.4\text{ V}$ vs Ag/AgCl), where hydrogen peroxide produced from the oxidation of glucose is oxidized, is applied to the GOx-immobilized GO electrode. Current responses on the successive addition of glucose are recorded. As shown in Figure 2, the positive current at the GOx covalently attached GO electrode increases with the gradually injection of glucose (blue line) whereas no oxidation current is obtained at the pristine GO/Pt electrode (pink line), confirming that the current response arises from the oxidation of hydrogen peroxide produced during the enzyme reaction rather than from the direct oxidation of glucose on the electrode.

The calibrated steady-current responses with respect to glucose concentration at the GOx–GO electrode are shown in the inset of Figure 2. The steady currents are linear up to 22 mM glucose at the GOx covalently attached GO electrode with 0.785 mm^2 geometric area (i.e., 28 mM/mm^2). The linear relationship is higher than the 15 mM required for practical use in the detection of blood glucose.

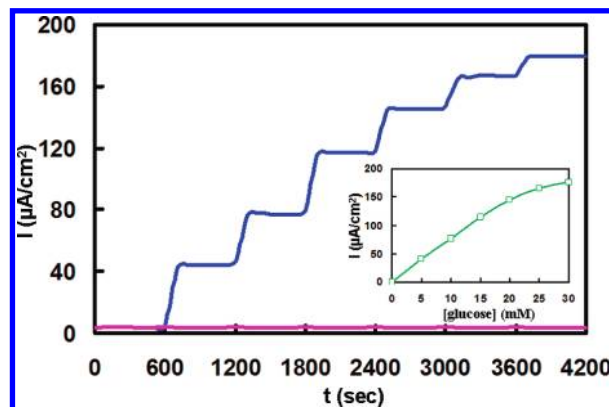


Figure 2. Typical amperometric responses at the GOx covalently immobilized GO electrode (blue line) and the pristine GO electrode (pink line) in 0.4 M PBS (pH 7.4) with the successive injection of 0, 5, 10, 15, 20, 25, and 30 mM glucose, respectively. (Inset) Calibration curve obtained for glucose determination at 0.4 V vs Ag/AgCl in 0.4 M PBS (pH 7.4).

The sensitivity of the enzyme electrode is determined by the slope of the calibration curve. The glucose oxidase covalently linked GO enzyme electrode exhibits a sensitivity of $8.045\text{ mA}\cdot\text{cm}^{-2}\cdot\text{M}^{-1}$. Considering that the content of GO in the resulting electrode is fairly low, the sensitivity obtained here is quite good.

Quartz crystal microbalance (QCM) measurements were used to determine the absorption stability of GO–GOx on the Pt electrode. A thin layer of GO was dropped onto the Pt probe of QCM. GOx was subsequently immobilized in GO as described above (Figure S1). The mass change can be determined by the Sauerbrey equation²³ (eq 1)

$$\Delta f = -2f_0^2 \Delta m / A(\mu_q \rho_q)^{1/2} \quad (1)$$

where Δf is the measured frequency shift, f_0 is the frequency of the quartz crystal prior to a mass change, Δm is the mass change, A is the piezoelectrically active area, μ_q is the shear modulus, and ρ_q is the density of quartz. The mass change is inversely related to the frequency shift. As shown in Figure 3, the frequency decreased slightly with the addition of GO onto the QCM probe, suggesting the low mass content of GO (from point 1 to 2, Figure 3). The frequency decreased significantly after the incorporation of GOx, indicating the successful immobilization of GOx onto GO (point 3). The frequency increased a bit after soaking GO–GOx in PBS solution for 1 day (point 4), suggesting the mass loss of the sample when soaking in PBS. This may be attributed to the loss of impurities such as unattached GOx, NHS, and EDC. The frequency remains stable even after soaking in PBS for 7 days (points 4–10), indicating the good stability of GO–GOx on the Pt probe. The sample was retained in air for several days, but the QCM frequencies remained quite stable, suggesting the strong anti-interference ability of GO–GOx/Pt.

Further evidence for the good stability of GO–GOx/Pt can be obtained using Raman spectroscopy (Figure S3). As expected, two well-known peaks at 1338 and 1560 cm^{-1} attributable to the D band (induced disorder) and the G band (the symmetric graphitic structure) of graphene²⁴ can be observed from the spectrum of pristine GO/Pt (blue line, Figure S3). The peak intensity ratio of the D band to the G band ($I_{D/G}$) is around 0.45, which is a bit higher than that of high-crystalline graphene sheets (normally

(21) Ramesha, G. K.; Sampath, S. J. *Phys. Chem. C* **2009**, *113*, 7986.

(22) Situmorang, M.; Gooding, J. J.; Hibbert, D. B.; Barnett, D. *Biosens. Bioelectron.* **1998**, *13*, 953.

(23) Buttry, D. A.; Ward, M. D. *Chem. Rev.* **1992**, *92*, 1355.

(24) Reina, A.; Jia, X.; Ho, J.; Nezich, D.; Son, H.; Bulovic, V.; Dresselhaus, M. S.; Kong, J. *Nano Lett.* **2009**, *9*, 30.

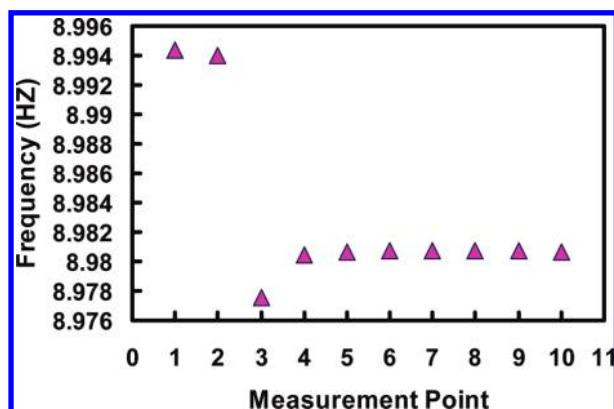


Figure 3. Data points from QCM measurements for (1) the pristine Pt tip, (2) the GO/Pt tip, (3) the GO–GOx/Pt tip, (4) the GO–GOx/Pt tip after soaking in PBS for 1 day, and (5–10) the GO–GOx/Pt tip after consecutive soaking in PBS for 2–7 days, respectively. All data were obtained after complete drying of the sample.

0.06–0.25).²⁴ The presence of oxygen-containing functional groups in GO gives rise to the relatively higher D band. Two well-defined peaks are still visible (pink line, Figure S3) after the incorporation of GOx, followed by soaking the GO–GOx/Pt in PBS (pH 7.4) over 7 days, confirming the presence of GO in the resulting enzyme electrode and the good stability of the nanosheet on the Pt electrode.

The reproducibility of the covalently attached GOx–GO electrode is evaluated using five enzyme electrodes prepared at identified conditions on different days. A relative standard deviation (RSD) of 5.8% was obtained, indicating the satisfied reproducibility of the resulting enzyme electrode for practical application. The storage stability is investigated using the GOx–GO enzyme electrode after having been stored in PBS (pH 7.4) at 4 °C for 1 month before biosensor testing. Only a 20% decrease in sensitivity was obtained. The decreased sensitivity may be attributed to the decline in enzyme activity. Therefore, the directly prepared GOx–GO enzyme electrode exhibits a wide linearity range, high sensitivity, excellent reproducibility, and good stability, suggesting potential applications in analyzing clinical samples over a wide range of physiological conditions.

We also carried out biocompatibility testing on the as-synthesized GO for the purpose of direct utilization of the resulting GO films as practical biodevices. Retinal pigment epithelium (RPE) is a neuroectodermal derivative that is essential to the survival of photoreceptors. In the present study, ARPE-19, a cell line derived from human RPE, was seeded onto the GO substrate. The cell nuclei were subsequently stained using 4', 6-diamidino-2-phenylindole (DAPI). DAPI is a fluorescent stain that binds strongly to DNA.

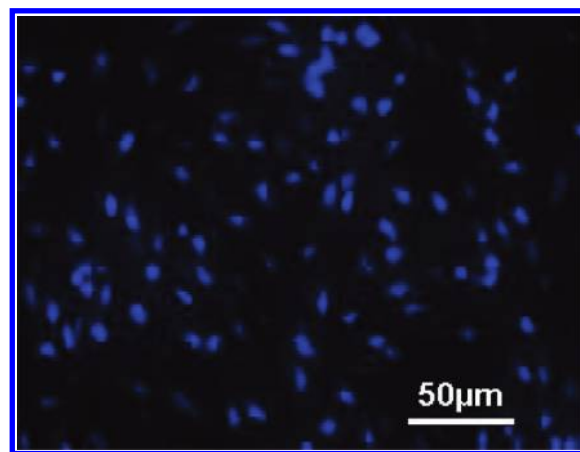


Figure 4. Fluorescence micrograph of DAPI-stained ARPE-19 cells growing on the GO film.

The good adhesion and differentiation of ARPE-19 cells on the GO film is visualized after 72 h of culture time as shown in the fluorescence micrograph in Figure 4, suggesting excellent biocompatibility of the as-prepared GO nanosheets.

Our preliminary work demonstrates the direct, efficient fabrication of glucose biosensors through the covalent attachment between carboxyl acid groups on GO sheets and the amine of GOx. The electrochemical performance of the GO electrode decreases after the introduction of GOx because of the weak electron-transferring nature of GOx. The covalently linked GOx–GO enzyme electrode shows broad linearity, good sensitivity, excellent reproducibility and storage stability, suggesting GO to be a highly efficient biosensor electrode. The good biocompatibility of the GO nanosheets has been illustrated, suggesting the direct application of the GO electrode on practical biological devices and in clinical diagnosis. The direct utilization of the functional groups of GO sheets opens up possibilities for the direct preparation of novel practical enzyme electrodes from graphene oxide for a wide range of applications, such as electrochemistry, biology, and biofuel cells.

Acknowledgment. ARPE-19 cells were kindly provided by Dr. Lin Hou (Wenzhou Medical College). Financial support from the Zhejiang Department of Education (grant no. Y200906587), the Ministry of Science and Technology of China (grant no. 2009DFB30380), and the Zhejiang Department of Science and Technology (grant no. 2009C13019) is acknowledged.

Supporting Information Available: Experimental details, cyclic voltammograms, and Raman spectra. This material is available free of charge via the Internet at <http://pubs.acs.org>.